Prediction of critical distance for tunneling with water-filled cavity ahead of tunnel face

Prévision de la distance critique pour les tunnels profonds avec une cavité remplie d'eau placée au front du tunnel

Changbing Qin, Siau Chen Chian
Department of Civil & Environmental Engineering, National University of Singapore, Singapore, sc.chian@nus.edu.sg

ABSTRACT: In tunnel engineering, precise prediction of face stability can be challenging due to various influencing factors, particularly when tunnels are excavated under water-filled cavities. In this paper, a newly postulated failure mechanism composing of two logarithmic spirals truncated by the boundary of a water-filled cavity was adopted to determine the critical distance between tunnel face and the cavity. The upper bound solution of minimal safe distance, which plays an important role in the design and construction of deep tunnels, was obtained using upper bound theorem and optimization. A parametric study on the effect of corresponding parameters on face stability was also carried out. Limit analysis method was conducted to offer an alternative to investigate the incipient failure of tunnel face, so as to provide guidance to similar tunneling operations.

RÉSUMÉ : En ingénierie des tunnels, il est assez compliqué d'effectuer une prédiction précise de la stabilité du front en raison de multiples facteurs, en particulier lorsque des tunnels sont creusés sous des cavités remplies d'eau. Dans ce cas, nous postulons qu'un nouveau mécanisme de défaillance composé de deux spirales logarithmiques tronquées par la limite de la cavité remplie d'eau peut être adopté pour déterminer la distance critique entre le front du tunnel et la cavité. Nous optimisons la solution de limite supérieure de la distance de sécurité minimale grâce au théorème de limite supérieure qui joue un rôle important dans la conception et la construction de tunnels profonds. L'effet des paramètres correspondants sur la stabilité du front est ensuite étudié. Les travaux présentés démontrent que la méthode d'analyse des limites offre une alternative pour étudier les risques d'effondrement du front du tunnel, fournissant ainsi des prévisions solides pour des projets similaires.

KEYWORDS: kinematic analysis; water-filled cavity; tunnel face stability; supporting pressure; critical distance

1 INTRODUCTION

The stability analysis and evaluation of ground surface settlement of tunnels induced by pressurized shield machinery are key to determining the success of the tunneling operation. The focus of stability analysis is placed on the derivation of minimal pressure stemmed from air, slurry or earth for ensuring tunneling safety. On the other hand, the analysis of surface displacements aims at estimating the pattern of surficial deformation due to tunneling. In some geological formation, tunneling operations may run the risk of encountering cavities saturated with water within the soil strata, which affects face stability. This paper discusses the face stability of a deep-buried tunnel with a circular profile in such ground conditions.

Face stability analysis in tunneling has been carried out by many researchers, such as Broms and Bennermark (1967), Kimura and Mair (1981), Ellstein (1986), Augarde *et al.* (2003), and Klar *et al.* (2007). A load factor N was introduced to evaluate the face stability of tunnels in a purely cohesive soil. This load coefficient N is defined as $N=(\sigma_s+\gamma H-\sigma_t)/c_u$, where σ_s =surcharge load imposed on the ground surface; γ =soil weight per volume; H =depth of the tunnel axis to the ground surface; σ_t = uniaxial tensile strength of soil; c_u =soil undrained cohesion. In the above literature, limit analysis, limit equilibrium and experimental approaches were applied to estimate the load factor. Kimura and Mair (1981) carried out centrifuge tests to obtain the value of N, ranging from 5 to 10, and is dependent on the tunnel's cover depth. On the basis of limit equilibrium method, Ellstein (1986) derived the analytic expression of N in homogeneous cohesive soil and the results were in good agreement with those obtained by Kimura and Mair (1981). Later, within the scope of plasticity theory, the kinematic method was used by Klar *et al.* (2007) who constructed an admissible velocity field in both planar and three-dimensional (3D) space. Through 3D analysis of face stability, the computation results were improved in some cases.

Experimental research, numerical and analytical approaches also have been broadly employed to investigate face stability of tunnels constructed in frictional soils. Chambon and Corté (1994) conducted centrifuge tests to describe the collapse mechanism and obtain the critical face pressure to avoid face collapse. That research shows that the collapse mode under limit state presents the shape of chimney and does not necessarily reach the ground surface. In this case, as widely acknowledged, the collapse mechanism is constructed by logarithmic spirals in the vertical cross-sections and elliptical shapes in the horizontal cross-sections, and thereafter numerical results can be worked out based on the given mechanism. In order to derive analytical solutions, limit equilibrium was applied by Anagnostou and Kovari (1996) and Broere (1998), using the same failure mechanism put forward by Horn (1961) to calculate the critical face pressure. However, the results were obtained based on priori assumptions with respect to the collapse shape and the normal stress distribution generated on the face of the collapsing block. Such a problem could also be investigated with the kinematic analysis approach so as to overcome the shortcoming of previous methods. Leca and Dormieux (1990) established a two-block failure mechanism for deriving more rigorous solutions of face stability.

The limit analysis approach, regarded as an analytical method, has been increasingly employed to evaluate the stability of tunnel face in frictional and/or cohesive soils. Mollon *et al.* (2009) proposed a translational 3D failure pattern composed of five conical moving blocks which enable the blocks to slide more freely, and the results were highly improved compared to those gained by Leca and Dormieux (1990). On the other hand, the region of failure in circular tunnel face was formed by an elliptical area, thus the remaining coverage of tunnel face would be inactive. In this case, a spatial discretization technique was developed to generate 3D failure surface by Mollon *et al.* (2010) in which the drawback could be overcome. Mollon *et al.* (2011)

then generated a rotational velocity discontinuous surface with the spatial discretization technique which showed that the intersection of a collapse mode for a circular tunnel is elliptic, implying that there exists an 'inclined' velocity field in the whole tunnel face.

At this juncture, the tunnel face stability in soil strata with condition of water-filled cavities has not been investigated thoroughly and will be the focus of this paper.

2 KINEMATIC ANALYSIS

This paper aims to derive the collapse pressure under limit state. As discussed, the kinematic analysis approach within the framework of plasticity theory is a sound choice to investigate the stability problems of tunnel face. The upper bound theorem states that the actual collapse load is no more than the load obtained by equating the rate of external work to the rate of internal energy dissipation in any kinematically admissible velocity field, when the deformation boundary is satisfied (Chen 1975).

$$\int_{\Omega}\sigma_{ij}\dot{\varepsilon}_{ij}d\Omega \geq \int_{\Omega}X_i v_i d\Omega + \int_{s}T_i v_i ds \tag{1}$$

where σ_{ij} and $\dot{\varepsilon}_{ij}$ are the stress tensor and strain rate at failure in a kinematically admissible collapse mechanism, respectively, T_i is the surcharge loading on the boundary s, X_i represents the body force, Ω is the volume of the impending failure block and v_i refers to the velocity along with the detaching surface. For simplification, the kinematic analysis is carried out based on the assumption of rigid geomaterials, requiring the soil material to comply with an associated flow rule and plastic.

The collapse occurred in front of tunnel face is induced by the self-weight of geomaterials and effect of water pressure in the case of cavities filled with water. Application of surcharge load has a direct effect when the failure mechanism outcrops at the ground surface. However, the analysis in this literature is related to face collapse for deep-buried tunnels, which implies the failure pattern does not necessarily attain to the ground surface, thus the effect of surcharge loading is ignored in the stability analysis.

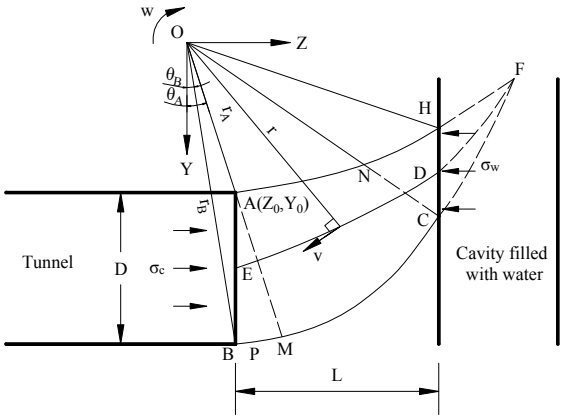

Figure 1. Failure mechanism with a water-filled cavity positioned ahead of tunnel face

Eisenstein and Ezzeldine (1994) proposed an axisymmetric and 3D model to evaluate the stability of a tunnel face. Meanwhile, it was generally adopted that the shape of collapse region is characterized by two logarithmic spirals with an opening angle equal to 2φ so as to satisfy the normality condition in limit analysis. Therefore, this paper applies the similar failure mechanism for the case of a cavity filled with water in front of tunnel face to analyze the effect of water pressure and determine the safe distance between the tunnel face and the edge of cave. Figure 1 describes the kinematically admissible velocity field which is a portion of entire failure mechanism presented in the existing study. This is arguable since the cave boundary is involved at failure, and therefore its velocity discontinuous line intersects at the borderline with water pressure imposed on the potential moving block.

The rotational mechanism emerges from A and B (i.e., the crown and invert of the tunnel face) with the same rotational center O. The corresponding equations in a polar (r,θ) coordinate system centered at O are expressed as

$$r_1 = r_A \exp\left[\left(\theta-\theta_A\right)\tan\phi\right] \tag{2}$$

$$r_2 = r_B \exp\left[\left(\theta_B-\theta\right)\tan\phi\right] \tag{3}$$

where r_1 and r_2 are the expressions of upper and lower logarithmic spiral, $r_A, r_B, \theta_A, \theta_B, Y_0, Z_0$ are illustrated in Figure 1, φ is the frictional angle of soil. On the margin of the cave closer to the tunnel face, the intersection of C and H can be described as

$$r_C\sin\theta_C = L + Z_0,\ \ r_H\sin\theta_H = L + Z_0 \tag{4}$$

where r_C, r_H are the radii at the intersections of C and H, θ_C, θ_H represent the angles with the vertical, L is the distance between the tunnel face and the edge of cave.

Based on the proposed failure mechanism, the computation of external work rate and internal energy dissipation is performed as follow. For deep-buried tunnels, the structure and stress distribution could be approximately regarded as axisymmetrical though there may exists an inclined angle of ground surface with respect to the horizontal.

Concerning the symmetry of tunnel structures, the work rate calculation generated by self-weight is divided into several parts. For a rotational failure mechanism, the magnitude of velocity in each infinitesimal body is proportional to the corresponding radius, i.e., $v = w r$ where r is the length of the gravity-center of the infinitesimal body to center O. The direction of velocity is normal to the radius vector. Given this proposed mechanism, it is subdivided into three sections and the detail calculation process is as shown below.

The triangle OBM is made up of triangle ABM and OAB, thus the work rate produced by soil weight in the region of ABM is equal to the difference of that calculated in the area of OBM and OAB. The self-weight work rate of OAB hence results in

$$\dot{W}_{\gamma\,OAB} = \gamma\left(w\frac{2}{3}r_A\sin\theta_A\right)\left(\frac{1}{2}r_A D\sin\theta_A\right) \tag{5}$$

The entire work rate of OBM can be expressed through integration over the interval $[\theta_B, \theta_A]$.

$$\dot{W}_{\gamma\,OBM} = \gamma\int_{\theta_B}^{\theta_A}\frac{1}{3}wr_2^3\sin\theta d\theta \tag{6}$$

Similarly, the external work rate induced by soil weight in $AMCN$ equals to the magnitude of self-weight work rate in

OMC less that in OAN. The expression in OMC is obtained through integration over the interval $[\theta_A, \theta_C]$, i.e.,

$$\dot{W}_{\gamma\ OMC} = \gamma \int_{\theta_A}^{\theta_C} \frac{1}{3} w r_2^3 \sin\theta \, d\theta \tag{7}$$

For section OAN, the overall self-weight contribution yields

$$\dot{W}_{\gamma\ OAN} = \gamma \int_{\theta_A}^{\theta_C} \frac{1}{3} w r_1^3 \sin\theta \, d\theta \tag{8}$$

Again, the work rate of HCN is the difference between that of OCH and ONH. In section OCH, the work rate is

$$\dot{W}_{\gamma\ OCH} = \gamma \left(w \frac{2}{3} r_C \sin\theta_C \right) \left[\frac{1}{2} r_C \sin\theta_C \left(r_C \cos\theta_C - r_H \cos\theta_H \right) \right] \tag{9}$$

Likewise, the corresponding solution of that in the sector ONH can also be obtained by integrating the work rate of infinitesimal body over $[\theta_C, \theta_H]$, which gives

$$\dot{W}_{\gamma\ ONH} = \gamma \int_{\theta_C}^{\theta_H} \frac{1}{3} w r_1^3 \sin\theta \, d\theta \tag{10}$$

As shown in Figure 1, the failure block is constituted by the above three sections, and the entire work rate of soil weight is the sum of those equations of $\dot{W}_\gamma$.

In the presence of a velocity discontinuity surface, the moving block would induce internal energy dissipation because of plastic deformation. There exists two velocity discontinuity lines, *BC* and *AH*. For the velocity detaching line *BC* belonging to the lower logarithmic spiral, the rate of internal energy dissipation gives

$$D_{BC} = c \int_{\theta_B}^{\theta_C} w r_2^2 \, d\theta = c\, w r_B^2 \frac{1 - \mathrm{e}^{2(\theta_B - \theta_c)\tan\phi}}{2\tan\phi} \tag{11}$$

Similarly, the energy rate dissipated along another velocity line, *AH*, results in

$$D_{AH} = c \int_{\theta_A}^{\theta_H} w r_1^2 \, d\theta = c\, w r_A^2 \frac{\mathrm{e}^{2(\theta_H - \theta_A)\tan\phi} - 1}{2\tan\phi} \tag{12}$$

Therefore, the total dissipated energy along the velocity detaching surfaces is the sum of above two equations.

In practice, it is often difficult to evaluate the collapse pressure of tunnel face due to the random variability of the mechanical properties of soils in situ and in the presence of fractures and cracks in the soil mass. It is worth noting that the collapse would not take place if the applied pressure is sufficient to support the impending block from moving towards the tunnel face. In this case, an effective approach is to provide a reasonable supporting pressure applied on the tunnel face. For simplification, the work rate of supporting pressure could be easily obtained with an assumption of uniform pressure distribution, i.e.

$$\begin{aligned} \dot{W}_{\sigma_c} &= -\sigma_c \int_{\theta_B}^{\theta_A} \left(w \frac{\sin\theta_A}{\sin\theta} r_A \cos\theta \right) \left(\frac{\sin\theta_A}{\sin\theta} r_A \frac{d\theta}{\sin\theta} \right) \\ &= w \sigma_c r_A^2 \frac{1}{2} \left(1 - \frac{\sin^2\theta_A}{\sin^2\theta_B} \right) \end{aligned} \tag{13}$$

where σ_c is the supporting pressure imposed on the tunnel face.

Encountering soils with several water-filled cavities, tunnels are more likely to fail. Considering the adverse water effect on tunnel stability, this effect should be considered and incorporated into the upper bound theorem. Water pressure is assumed to be uniformly distributed herein. In this case, the work rate of water pressure yields

$$\begin{aligned} \dot{W}_{\sigma_w} &= \sigma_w \int_{\theta_C}^{\theta_H} \left(w \frac{\sin\theta_H}{\sin\theta} r_H \cos\theta \right) \left(\frac{\sin\theta_H}{\sin\theta} r_H \frac{d\theta}{\sin\theta} \right) \\ &= w \sigma_w r_H^2 \frac{1}{2} \left(\frac{\sin^2\theta_H}{\sin^2\theta_C} - 1 \right) \end{aligned} \tag{14}$$

where σ_w is water pressure.

In order to compute the minimal supporting pressure for the prevention of potential failure blocks, an objective function composed of internal energy dissipation and external work rate is established. Theoretically, there exist infinite upper bound solutions for each problem; however, only one optimal solution can be reached when the objective function equals to zero under a set of given conditions, i.e.,

$$D = \dot{W}_\gamma + \dot{W}_{\sigma_c} + \dot{W}_{\sigma_w} \tag{15}$$

Substituting the above expressions of internal and external work rates into Eq. (15), the minimal supporting pressure can be obtained under the geometrical constraints. The restricted conditions imposed are:

$$0 < \theta_A < \pi/2,\ 0 < \theta_B < \pi/2,\ \theta_B < \theta_A,\ r_A < r_B \tag{16}$$

3 NUMERICAL RESULTS

3.1 *Upper bound solutions of supporting pressure*

In order to interpret the water effect on face stability, the numerical results under given parameters are calculated in this section. Six variables including tunnel diameter, cohesion, soil self-weight, frictional angle, water pressure acting on the potential block in front of tunnel face, and distance between tunnel face and water-filled cavity are investigated. Table 1 shows numerical solutions of the supporting pressure applied on the tunnel face to maintain face stability.

It can be observed in Table 1 that the supporting pressure increases: 1) with the increment in D, σ_w, γ, and 2) with the decreasing values of c_0, φ, and L. In this case, in order to minimize the construction work, tunnels are suggested to excavate in soils with high quality and far away from water-filled cavities. Parametric study could well shed light upon the failure mechanism under certain conditions and instruct the design and construction of underground structures.

3.2 *Upper bound solutions of critical distance*

In the initial excavation of tunnels, internal lining is not exerted or unable to provide the supporting pressure for resisting the potential sliding block. Under this circumstance, determination

of critical distance between the tunnel face and the cavity is of overriding significance to ensure the safety of tunnel construction. Based on the preceding analysis, the numerical results can be computed by optimization under given parameters, and the results as shown in Table 2.

Table 1. Values of supporting pressure under specific conditions

D/m	σ_w/kPa	c_0/kPa	γ/kN·m	φ/°	L/m	σ_c/kPa
10	200	50	25	15	3	147.87
9	200	50	25	15	3	140.82
8	200	50	25	15	3	131.73
10	180	50	25	15	3	131.41
10	160	50	25	15	3	114.95
10	140	50	25	15	3	98.49
10	200	60	25	15	3	141.27
10	200	70	25	15	3	134.66
10	200	80	25	15	3	128.06
10	200	50	25	15	3	147.87
10	200	50	22.5	15	3	146.24
10	200	50	20	15	3	144.61
10	150	50	20	9	3	113.98
10	150	50	20	15	3	103.46
10	150	50	20	21	3	92.16
10	200	50	20	15	4	127.43
10	200	50	20	15	5	110.07
10	200	50	20	15	6	92.12

Table 2. Upper bound solutions of critical distance

D/m	σ_w/kPa	c_0/kPa	γ/kN·m^{-3}	φ/°	L/m
15	150	50	25	15	7.99
18	150	50	25	15	20.47
20	150	50	25	15	26.24
15	120	50	25	15	7.99
15	150	50	25	15	7.99
15	200	50	25	15	7.99
15	150	45	25	15	14.35
15	150	47	25	15	12.30
15	150	50	25	15	7.99
15	150	50	25	15	7.99
15	150	50	26	15	10.99
15	150	50	27	15	13.07
15	150	50	25	14	9.93
15	150	50	25	15	7.99
15	150	50	25	16	5.73

It can be noted from Table 2 that the critical distance is affected by quantities D, c_0, γ and φ. The direct effect of water effect is minimal and may be neglected since it no longer applied on the potential failure block. As observed, the increase in D and γ leads to the longer critical distance. However, this effect reduces non-linearly with the increasing values of c_0 and φ. This places importance to ascertain these properties in the field, so as to safeguard the safety of tunnel operations.

4 CONCLUSION

The effect of water-filled cavities in tunneling has been discussed. A novel failure mechanism was postulated with two log spirals truncated by the boundary of the cavity. Based on the mechanism, the internal energy dissipation and external work rates were presented, and the upper bound solution of the required supporting pressure optimized within the framework of plasticity theory. Subsequently, sensitivity analysis was conducted to estimate the effect of relevant parameters on supporting pressure. The results indicate that larger c_0, φ, L, and lower D, σ_w, γ are beneficial to maintain face stability. Similarly, the critical distance between the tunnel face and cavity was determined under specific soil parameters, providing some guide on the estimates of the working conditions to ensure stability of the tunneling operation.

5 REFERENCES

Anagnostou G. and Kovari K. 1996. Face stability conditions with earth -pressure-balanced shields. *Tunn. Undergr. Space Technol.* 11(2), 165-173.

Augarde C.E. Lyamin A.V. and Sloan S.W. 2003. Stability of an undrained plane strain heading revisited. *Comput. Geotech.* 30, 419-430.

Broere W. 1998. Face stability calculation for a slurry shield in heterogeneous soft soils. *Proceedings of the World Tunnel Congress 98 on Tunnels and Metropolises*, Rotterdam, pp. 215-218.

Broms B.B. and Bennermark H. 1967. Stability of clay at vertical openings. *Soil Mech. Found. Eng.* (*Engl. Transl.*) 193(SMI), 71-94.

Chambon P. and Corté J.F. 1994. Shallow tunnels in cohesionless soil: stability of tunnel face. *J. Geotech. Eng.* 120(7), 1148-1165.

Chen W.F. 1975. *Limit Analysis and Soil Plasticity*. Elsevier Science, Amsterdam, Netherlands.

Eisenstein A.R. and Ezzeldine O. 1994. The role of face pressure for shields with positive ground control. *Tunnelling and Ground Conditions*, Balkema, Rotterdam, 557-571.

Ellstein A.R. 1986. Heading failure of lined tunnels in soft soils. *Tunnels and Tunnelling* 18, 51-54.

Horn N. 1961. Horizontaler erddruck auf senkrechte abschlussflächen von tunnelröhren. Landeskonferenz der ungarischen tiefbauindustrie, Landeskonferenz der Ungarischen Tiefbauindustrie, Budapest, Hungary 7-16.

Kimura T. and Mair R.J. 1981. Centrifugal testing of model tunnels in clay. *Proceedings of the 10th International Conference on Soil Mechanics and Foundation Engineering*, Rotterdam, pp. 319-322.

Klar A. Osman A.S. and Bolton M. 2007. 2d and 3d upper bound solutions for tunnel excavation using 'elastic' flow fields. *Int. J. Numer. Anal. Meth. Geomech.* 31(12), 1367-1374.

Leca E. and Dormieux L. 1990. Upper and lower bound solutions for the face stability of shallow circular tunnels in frictional material. *Geotechnique* 40(4), 581-606.

Mollon G. Dias D. and Soubra A.H. 2009. Probabilistic analysis and design of circular tunnels against face stability. *Int. J. Geomech.* 9(6), 237-249.

Mollon G. Dias D. and Soubra A.H. 2010. Face stability analysis of circular tunnels driven by a pressurized shield. *J. Geotech. Geoenviron. Eng. (ASCE)* 136(1), 215-229.

Mollon G. Dias D. and Soubra A.H. 2011. Rotational failure mechanisms for the face stability analysis of tunnels driven by a pressurized shield. *Int. J. Numer. Anal. Meth. Geomech.* 35, 1363-1388.